Proceedings of the 2011 International Conference on
Advanced Mechatronic Systems, Zhengzhou, China, August 11-13, 2011

Positioning Control Strategy Design for AFM Based Nanomanipulation Systems

Yongchun Fang, Xiao Ren, Yudong Zhang

Abstract— **An atomic force microscope (AFM) has been utilized to implement various manipulations with nanometer precision. Unfortunately, an AFM-based nanomanipulation system often meets the problem of low reliability and low efficiency, mainly due to the difficulty of positioning the AFM tip near the sample. In this study, a positioning control strategy is designed to accurately drive the probe to implement nanomanipulation tasks. Specifically, for an AFM piezo-scanner, a novel control strategy consisting of the following three algorithms are proposed to alleviate positioning error caused by such factors as piezo-hysteresis, cross-coupling and other uncertainties: (a) an image-based hysteresis compensation algorithm, which first obtains the voltage-displacement relationship of the hysteresis for the AFM piezo-scanner by analyzing some collected images for a calibration grating, and then utilizes this relationship to compute suitable control inputs to compensate for the positioning error caused by hysteresis nonlinearity; (b) a landmark-based positioning algorithm addressing cross-coupling effect, which first indents the sample to make regular landmarks by a series of control voltages, based on which a polynomial curve fitting method is then utilized to calculate proper inputs so that cross-coupling effect can be compensated efficiently; (c) a local scannning-based compensator, which addresses the positioning error caused by thermal drift or other uncertainties within the nanomanipulation system successfully. Some experiment results are included to show that precise nanopositioning performance can be achieved by using the presented approach.**

I. INTRODUCTION

The invention of atomic force microscope (AFM) brings great progress for nanoscience and nanotechnology [1]. Besides the main applications of nanoimaging, recently, an AFM is more and more utilized as a manipulating tool to operate objects in nanometer scale directly [2]. Compared with other nanomanipulation systems, AFM can manipulate various types of samples under different environments, such as UHV, air, fluid, and so on. Therefore, an AFM plays an important role in nanoscience and nanotechnology, and the concerned research of AFM nanomanipulation technique has been a hot topic in the mechatronics and robotics field.

In AFM-based nanomanipulation systems, how to accurate position the tip at the desired location is a key factor for the success of manipulation tasks. Unfortunately, some inherent factors in the system, such as thermal drift, cross-coupling effect in different motion directions, and the complex characteristics of nano-actuator including hysteresis, structural vibration and creep [3], bring much difficulty for accurate positioning. Besides, the positioning accuracy is also affected by the cross-coupling of the 3-dimensional nano-positioner. Thus, in order to enhance the system performance, many efforts have been devoted to alleviate these problems from the modeling and control point of view. For instance, to reduce the hysteresis nonlinearity, in [4], Tan *et al.* model the hysteresis nonlinearity by using extended input space neural network and then propose an inverse model to decrease its effect. However, as pointed out in [5], the performance of these inversion-based approaches usually depends largely on the model precision and is also sensitive to the parameters. Thus, many control scientists try to bring the feedback control into nanopositioning systems. Under this situation, the hysteresis-preceded input should be strictly considered, which then increases the difficulty of controller design and stability analysis. In order to solve this problem, adaptive control [6] and robust control [7] are proposed by considering the hysteresis with certain uncertainty. Furthermore, in [8], Liaw *et al.* combine robust and adaptive control algorithms to enhance the motion tracking performance of piezoelectric actuation systems for micro/nano manipulation. Besides, due to the long operation time in some nanomanipulation tasks, the creep phenomenon of the piezo-actuator becomes evident and thus has to be compensated efficiently. In [9], Requicha utilizes inverse model to compensate for creep and hysteresis simultaneously. Moreover, with the increasing of the operation time and the system temperature, thermal drift will further degrade the spatial positioning performance. To make it even worse, it is usually difficult to obtain an explicit model to describe the drift effect. Thus, most research employ predictive mechanisms, such as Kalman filter [10], neural network [11], and so on, to address this phenomenon.

However, with the decreasing of the scale of the manipulated object, the measuring noise of the nano-sensor will be unneglectable, which then makes the feedback control inefficient. Besides, the thermal drift cannot be easily observed by any nano-sensors. Considering this point, visual servoing is brought to supply realtime visual feedback for nanomanipulation systems [12]. Unfortunately, to ensure the validity of vision sensors, the size of the manipulated particles should be large enough ($4.5\mu m$ in [12]), which further limits its applications. Instead of the utilization of optical microscopes, in [13], the authors employ fault detection and correction technique to offer real-time videolization for nanomanipulations. However, it puts emphasis on the compensation of thermal drift without much consideration for the hysteresis nonlinearity.

Summarizing the existing results, it can be seen that most

This work was supported by National Natural Science Foundation of China (60875055) and the National High Technology Research and Development Program ("863" Program) of China (2009AA043703)

All the authors are with the Institute of Robotics and Automatic Information System (IRAIS), Nankai University, Tianjin, China. yfang@robot.nankai.edu.cn

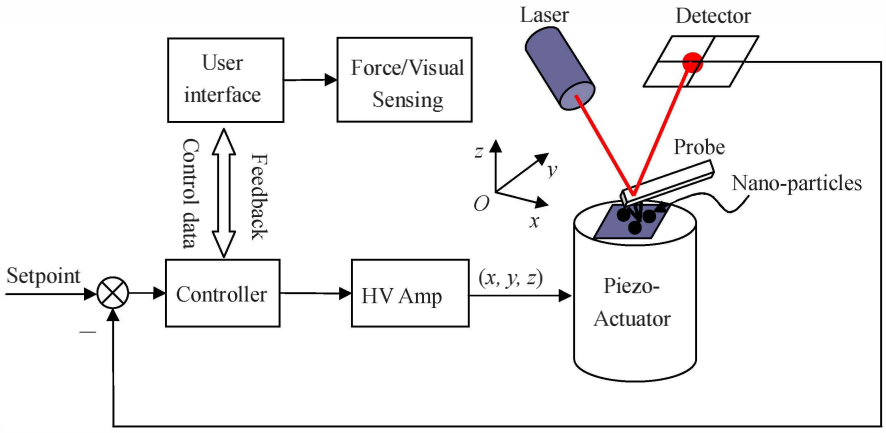

Fig. 1. Block diagram of AFM-based nanomanipulation systems

research has not studied the nanopositioning problem from a more comprehensive viewpoint covering all the influencing factors. Therefore, it is still an open problem to position the manipulator precisely in AFM-based nanomanipulation systems. In order to increase the AFM probe positioning accuracy, this paper considers the overall system nonlinearities and uncertainties, and it proposes a three-step positioning control strategy, which fully uses the available AFM image instead of any additional nano-sensors, to drive the probe to the desired location. Specifically, an image-based modeling and compensation algorithm is firstly presented to alleviate the hysteresis effect; Secondly, the cross-coupling effect caused positioning error is suppressed by a landmark-based compensator; Finally, for the remaining system uncertainties, the local scanning method is used to achieve precise positioning. The proposed control technique is verified by some experiment results. It is shown that this algorithm can ensure accurate positioning effectively.

The remainder of this paper is organized as follows. Section II briefly introduces the basic working principles of AFM-based nanomanipulation systems. Section III describes the design procedure of the proposed three-step positioning algorithm in details. Some experiment results are included in section IV to demonstrate the performance of the presented method. Finally, section V summarizes this work.

II. FUNDAMENTALS OF AFM-BASED NANOMANIPULATION SYSTEMS

As shown in Fig. 1, a typical AFM-based nanomanipulation system is composed of several key components including the main body of an AFM, controller, user interface and visual/force feedback device, and so on. Through this system, several manipulation tasks can be conducted, such as nanoindentation, nanopushing, nanoimprinting, and so on. Generally, the manipulation process includes four steps: driving the probe close to the surface of the sample, making the probe contact with the manipulated objects, completing the desired operation, leaving the probe from the sample. For instance, Fig. 2 shows a schematic process of pushing a nanoparticle. Specifically, the following four steps are carried out to accomplish the pushing task.

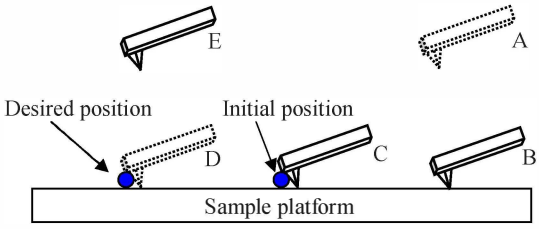

Fig. 2. Schematic diagram of pushing manipulation

A-B: In the beginning, the probe is far from the sample. It is driven to approach to the sample surface at a comparatively small distance so that the atomic force will be dominant between the probe and the sample. Moreover, the interaction force is regulated at setpoint under the feedback control in z-axis.

B-C: The probe is moved slowly in x-y plane to ensure that the probe gets contact with the manipulated particle.

C-D: With the precise control in both x-y plane and z-axis, the sample is pushed by the probe to track the predesigned trajectory until it reaches the desired position.

D-E: Retracing the probe away from the sample, and the overall pushing process is completed.

It should be noted that, in the previous nanomanipulation process, whether the objective can be achieved successfully depends strongly on the positioning control in x-y plane and force control in z-axis. In this research, the former control issue is carefully studied, and a positioning strategy is presented in the subsequent section.

III. POSITIONING ALGORITHM DESIGN

This section presents a precise positioning strategy to drive the probe to the desired location. It is further separated into three steps to deal with different positioning errors: inversion-based hysteresis compensation, landmark-based coarse positioning, and accurate positioning by the local-scan method.

A. Inversion-based Hysteresis Compensation

A piezo-actuator is widely utilized in an AFM system to provide 3-dimensional displacements. As a dominant actuator in micro/nano fields, it has superior performance, such as high resolution, fast response, large stiffness, and so on. Unfortunately, its input-output relationship presents multiple-valued nonlinear hysteresis characteristic, which largely decreases the positioning accuracy. Moreover, it is usually difficult to appropriately model hysteresis and then compensate it.

Preisach model is the mostly utilized model to describe the hysteresis for its high resolution [14]. It is generally expressed as:

$$d(t) = \Gamma(u)(t) \triangleq \int \int_{\alpha \geq \beta} \mu(\alpha, \beta) \gamma_{\alpha\beta}[u(t)] d\alpha d\beta \qquad (1)$$

where $u(t)$ denotes the input voltage, $d(t)$ represents the output displacement, with $\gamma_{\alpha\beta}[u(t)]$ and $\mu(\alpha, \beta)$ being the hysteresis operator and corresponding weight respectively.

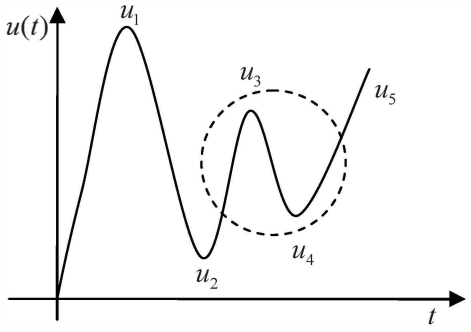

Fig. 3. Wiping out property of Preisach model

However, the identification of model parameters is rather complicated. In this research, considering the wiping out property [15] of Preisach model and the actual range in nanomanipulation tasks, we employ an image-based single cycle compensation approach. As shown in Fig. 3, in an input sequence $\{u_1, u_2, u_3, u_4, u_5\}$, if $u_1 > u_3$ and $u_2 < u_4$, then the final output corresponding with input u_5 is only related to u_1, u_2 and u_5, while u_3 or u_4 has no effect on the final output. That is,

$$d(t) = \Gamma[u](t) \approx f(u_1, u_2, u_5). \qquad (2)$$

Therefore, for a given manipulation range, without the consideration of other factors, such as thermal drift and creep, the output displacement can be regarded as repeatable. In that way, the ascending and descending curves are all determined. Then, in a specific manipulation task, the range $[u_2, u_1]$ is firstly appointed as the minimum and maximum values of the input voltage. And, before the manipulation, the piezo-actuator is excited by input $\{u_2, u_1\}$ to initial it to ensure that the same condition is always achieved.

Based on the wiping out property, the single cycle input-output relationship is obtained by scanning calibration grating with known period and analyzing the image data [16]. Then, the hysteresis can be compensated according to this relationship. Specifically, the algorithm is implemented in the following steps:

1) Imaging the calibration grating within the predefined manipulation range. In order to avoid the influence of scanning speed on hysteresis, the scanning frequency is chosen to be under 1Hz;

2) Analyzing the AFM image of the standard sample and extracting the feature points. In this step, the input/output data is further fitted into the form of polynomials by using least square method;

3) Calculating the compensating input. Since the above polynomial is usually ill-conditioned, neural network (NN) is employed in this research to train the desired input. During the training process, the output displacement and the input voltage are set as the input layer and the output layer. Then the relationship of displacement-voltage can be obtained by this inversion method.

4) Exerting the input sequence on the piezo-actuator. Based on the NN obtained in 3), the specific input sequence is calculated, and then exerts on the piezo-actuator to compensate for the hysteresis nonlinearity.

B. Landmark Based Coarse Positioning

Besides the hysteresis nonlinearity, the positioning deviation is also caused by cross-coupling, creep, and some other uncertainties, which are expressed as synthesis error. Different from hysteresis, the synthesis error is more difficult to describe by a mathematical model and it can not be observed by a nano-sensor. Thus, the compensation for the synthesis error cannot be easily achieved by either model-based feedforward or sensor-based feedback control method.

Based on the previous analysis, a landmark-based positioning method is proposed in this paper to coarsely drive the probe to the desired location. The basic idea of this approach is imprinting the sample surface in the manipulation space in accordance with the predesigned sequence. Since the imprinted area represents where the probe actually reaches and the input voltage is exactly known, after obtaining and then analyzing a number of imprinted points, the corresponding relationship between the actual and desired positions can be obtained. When positioning the probe in the manipulation task, this relationship can be used to compensate for the synthesis error, and to ensure that the probe moves near the desired position.

Specifically, the landmark-based compensation method includes the following steps:

1) $N \times N$ points are imprinted on an AFM image. Assuming that the image resolution is $n \times n$, then the starting point of these points (P_x, P_y) and the step length S of the imprinting process should satisfy:

$$\begin{aligned} P_x + S \times (N-1) &< n \\ P_y + S \times (N-1) &< n \end{aligned} \qquad (3)$$

According to the above imprinting setup, the desired positions of these printed points can be determined, which is

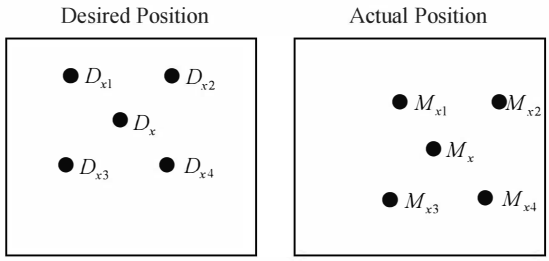

Fig. 4. Landmark based interpolation algorithm

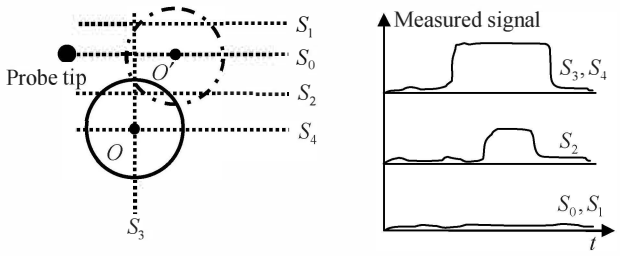

Fig. 5. Local scanning method

denoted as D_{NN} for the subsequent analysis. Then, the input sequence after the compensation for hysteresis is calculated by employing the method described in subsection III-A. To facilitate the following compensation algorithm, it is expressed as I_{NN}.

2) The imprinted area is re-scanned by an AFM to obtain the image after imprinting. By using some image processing methods, the coordinate of each imprinted point is extracted, which is further expressed as M_{NN} denoting the actual position of the probe under the exertion of the input sequence I_{NN}.

3) The imprinted points is used as landmarks for the compensation of the synthesis error. Taking the x axis as an instance to depict the compensation algorithm. As shown in Fig. 4, (M_x, M_y) is set as the desired position of the probe. Then several feature points around it can be easily found as well as their original desired positions, which are denoted as M_{xi} and D_{xi}, $i = 1, \cdots, m$ respectively, where m is the number of the feature points ($m = 4$ in Fig. 4). Furthermore, by comparing the relationship between D_{NN} and I_{NN}, the corresponding inputs are obtained as I_{xi}, $i = 1, \cdots, m$. Based on these feature points, the following interpolation method is employed to estimate the actual input coordinate I_x:

$$I_x = \frac{2}{m(m-1)} \sum_{i,j} f_{ij} \tag{4}$$

where

$$f_{ij} = \frac{M_x - M_{xi}}{M_{xj} - M_{xi}} (I_{xj} - I_{xi}) + I_{xi} \tag{5}$$

with $1 \leq i < j \leq m$, $m \geq 2$.

It should be noted that, this landmark based compensation approach can deal with the control error of the hysteresis as well as the synthesis error. Through this method, the probe can be positioned roughly at the desired location. However, considering the error of extracting feature points and the thermal drift in the mechanical system, the local scanning technique will be further used to accurate drive the probe to reach the desired position.

C. Local Scanning Based Accurate Positioning

After the utilization of the inversion based hysteresis compensation and landmark based correction of synthesis error, the probe is positioned very near the manipulated object. To guarantee accurate manipulation, a small range scan is then taken to ascertain the precise position [13].

Specifically, as shown in Fig. 5, suppose that the nanoparticle is located at $O(x, y)$, and its radius is $R \in \mathbb{R}^+$, which can be determined by the pre-scanning image. Besides, the probe tip is aligned with $O'(x, y)$ in y axis. Then the local scanning method is conducted in the following procedures to obtain the accurate position of the particle $O(x, y)$:

1) Seeking the sample in the x direction: The probe is scanned along the x axis to obtain a scan line S_0. If a big fluctuation appears in this line, which implies that the probe contacts with the sample, then turn to the second step 2); else, scan the sample around S_0 with a distance of $0.75R$, until find the particle.

2) Seeking the sample in the y direction: In the right plotting of Fig. 5, neither S_0 nor S_1 finds the particle. Assume that the particle is found by the scan line S_2. Then, the middle position of the fluctuation in S_2 is calculated, based on which some scans along the y axis are further implemented to determine the center position of the particle $O(x, y)$.

3) Result verification: To ensure that the right sample, instead of other objects is found by the scan line, another scan is implemented to make the judgement by utilizing the sample size as *a priori*. For this purpose, starting from the center position of the particle O, scan the sample, if the pulse width is similar with the particle diameter $2R$ (generally, the difference is less than 10%), then the positioning task succeeds; otherwise, repeat the previous steps.

IV. EXPERIMENT RESULTS

To verify the performance of the presented positioning algorithm in section III, some experiments are conducted in the homemade AFM-based open nanomanipulation platform. In this testbed, based on the Benyuan CSPM4000 AFM microscope, a RTLinux based realtime nanomanipulation system is developed [17], in which the hysteresis compensation, landmark based coarse positioning and local scanning are integrated.

For the three-step positioning strategy, the hysteresis nonlinearity is first identified by imaging a standard sample with known period (depicted by Fig. 6) and extracting the feature points to obtain the input-output relationship. Then, the compensated input is calculated according to this relation. Fig. 7 shows the AFM image of calibration grating after

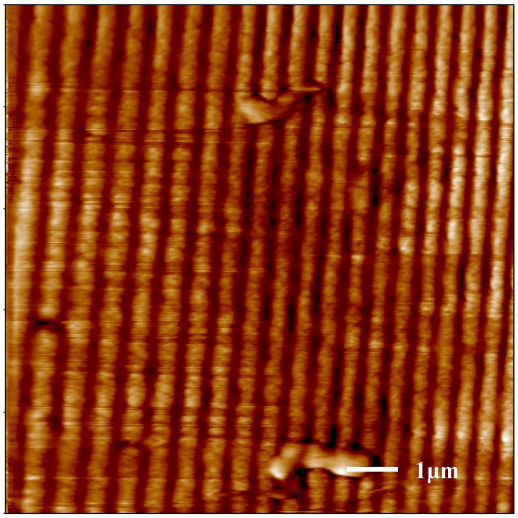

Fig. 6. AFM image of calibration grating without compensation

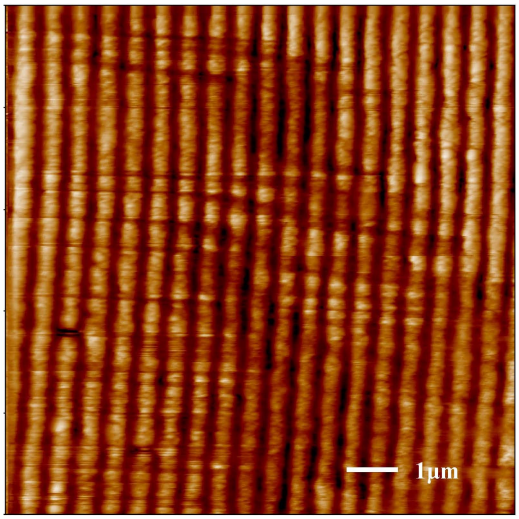

Fig. 7. AFM image of calibration grating after compensation

compensation for hysteresis. Compared with Fig. 6, the periodic property is well maintained with compensation, which is in agreement with the real sample surface.

Subsequently, the landmark-based coarse positioning and local scanning algorithms are conducted to accurate drive the probe at desired location. Finally, a pushing experiment for nanoparticles is carried out in order to validate its effectiveness. The result demonstrates that the particle is manipulated successfully, which then infers that the presented algorithm enhances the nanopositioning performance remarkably.

V. CONCLUSION

This paper studies the positioning control issue of a piezo-actuator for accurate nanomanipulation. The hysteresis nonlinearity is firstly analyzed and then compensated by utilizing the wiping out property of classical Preisach model. Subsequently, the landmark-based coarse positioning and local scanning algorithms are employed respectively to deal with the synthesis error and the positioning error caused by thermal drift. Experiment results indicate that the three-step precise control approach can accurately drive the probe to the desired location, which then facilitates the subsequent nanomanipulation tasks.

REFERENCES

[1] G.Binnig, C. Quate, "Atomic Force Microscope", *Physical Review Letters*, Vol. 56, No. 9, pp. 930-934, 1986.

[2] M. Sitti, "Survey of Nanomanipulation Systems", *IEEE Conference on Nanotechnology*, Maui, USA, Oct. 28-30, 2001, pp. 75-80.

[3] D. Croft, G. Shed, and S. Devasia, "Creep, Hysteresis, and Vibration Compensation for Piezoactuators: Atomic Force Microscopy Application", *ASME Journal of Dynamic Systems, Measurement, and Control*, Vol. 123, No. 1, pp. 35-43, 2001.

[4] X. Zhao, Y. Tan, "Modeling Hysteresis and its Inverse Model Using Neural Networks Based on Expanded Input Space Method", *IEEE Transactions on Control Systems Technology*, Vol. 16, No. 3, pp. 484-490, 2008.

[5] S. Devasia, E. Eleftheriou, and S. O. R. Moheimani, "A Survey of Control Issues in Nanopositioning", *IEEE Transactions on Control Systems Technology*, Vol. 15, No. 5, pp. 802-823, 2007.

[6] X. Chen, T. Hisayama, C. Su, "Adaptive Control for Continuous-Time Systems Preceded by Hysteresis", *47th IEEE Conference on Decision and Control*, Cancun, Mexico, 2008, pp. 1931-1936

[7] C. Lee, S. M. Salapaka, "Robust Broadband Nanopositioning: Fundamental Trade-offs, Analysis, and Design in a Two-Degree-of-Freedom Control Framework", *Nanotechnology*, Vol. 20, No. 3, p. 35501, 2009.

[8] H. C. Liaw, B. Shirinzadeh, J. Smith, "Robust Adaptive Motion Tracking Control of Piezoelectric Actuation Systems for Micro/Nano Manipulation", *2007 IEEE International Conference on Robotics and Automation*, Roma, Italy, Apr. 10-14, 2007, pp. 1110-1115.

[9] B. Mokaberi, A. A. G. Requicha,"Compensation of Scanner Creep and Hysteresis for AFM Nanomanipulation", *IEEE Transactions on Automation Science and Engineering*, Vol. 5, No. 2, pp. 197-206, 2008.

[10] B. Mokaberi, A. A. G. Requicha, "Drift Compensation for Automatic Nanomanipulation with Scanning Probe Microscopes", *IEEE Transactions on Automation Science and Engineering*, Vol. 3, No. 2, pp. 199-207, 2006.

[11] Q. Yang, S. Jagannathan, and E. W. Bohannan, "Automatic Drift Compensation Using Phase Correlation Method for Nanomanipulation", *IEEE Transactions on Nanotechnology*, Vol. 7, No. 2, pp. 209-216, 2008.

[12] C. D. Onal, M. Sitti, "Visual Servoing-Based Autonomous 2-D Manipulation of Microparticles Using a Nanoprobe", *IEEE Transactions on Control Systems Technology*, Vol. 15, No. 5, pp. 842-852, 2007.

[13] L. Liu, Y. Luo, N. Xi, Y. Wang, J. Zhang, G. Li, "Sensor Referenced Real-Time Videolization of Atomic Force Microscopy for Nanomanipulations", *IEEE/ASME Transactions on Mechatronics*, Vol. 13, No. 1, pp. 76-85, 2008.

[14] A. Visintin. "Differential Models of Hysteresis", Berlin: Springer, 1994.

[15] I. D. Mayergoyz, "Mathematical Models of Hysteresis", New York: Springer-Verlag, 1991.

[16] Y. Zhang, Y. Fang, X. Zhou, X. Dong, "Image-Based Hysteresis Modeling and Compensation for an AFM Piezo-Scanner", *Asian Journal of Control*, Vol. 11, No. 2, pp. 166-174, 2009.

[17] X. Zhou, Y. Fang, X. Dong, Y. Zhang, "Real-time Feedback Control System for AFM Based on RTLinux", *Computer Engineering*, Vol. 34, No. 15, pp. 226-228, 2008.